ESC European Heart Journal - Digital Health (2026) 7, ztag024
https://doi.org/10.1093/ehjdh/ztag024

ORIGINAL ARTICLE

Artificial intelligence-powered automatic coronary computed tomography angiography plaque quantification: comparison against optical coherence tomography

Guanyu Li[1,†], Wei Yu[1,†], Zhiqing Wang[1,2], Yankai Chen[1], Miao Chu[1,*], Zehang Li[3,4], Chunming Li[1], Xiaoling Wang[1], Yuanming Yan[2], Yukun Luo[2], Wei Cai[2], Giovanni Luigi De Maria[5], Charalambos Antoniades[5], Adrian Banning[5], Lianglong Chen[2], and Shengxian Tu[1,5,6,*]

[1]Biomedical Instrument Institute, School of Biomedical Engineering, Shanghai Jiao Tong University, Shanghai 200030, China; [2]Department of Cardiology, Fujian Medical University Union Hospital, Fuzhou, China; [3]Department of Radiology, Shanghai Jiao Tong University Affiliated Ruijin Hospital, Shanghai, China; [4]College of Health Science and Technology, Shanghai Jiao Tong University School of Medicine, Shanghai, China; [5]Division of Cardiovascular Medicine, Radcliffe Department of Medicine, University of Oxford, Oxford, UK; and [6]Institute of Medical Robotics, Shanghai Jiao Tong University, Shanghai, China

Received 11 June 2025; revised 10 July 2025; accepted 5 January 2026; online publish-ahead-of-print 9 February 2026

Aims Coronary computed tomography angiography (CCTA) enables a non-invasive, comprehensive assessment of coronary artery disease, and artificial intelligence (AI) offers the potential to improve CCTA image interpretation. This study aimed to evaluate the performance of an AI-powered method for automatic plaque quantification from CCTA, with optical coherence tomography (OCT) as reference standard.

Methods and results Patients who underwent CCTA within 6 months prior to OCT were retrospectively enrolled. AI-assisted automatic plaque quantification was performed on CCTA with specific plaque composition classification based on adaptive Hounsfield unit thresholds. Qualitative high-risk plaque features were also assessed. Automated co-registration of CCTA and OCT was performed with the link of invasive coronary angiography. A total of 91 patients with 153 co-registered lesions were evaluated. The AI-assisted automatic CCTA analysis showed significant correlations with OCT for quantifying plaque volume/burden and different plaque compositions (all P values <0.001); of which, the correlation coefficient for plaque volume was 0.84. Vulnerable plaque, defined as lipid-to-cap ratio >0.33 on OCT, was identified in 39 (25.5%) lesions. CCTA-derived plaque volume >82.5 mm^3 [odds ratio (OR), 9.39], maximal plaque burden >76.4% (OR, 3.70), lipidic tissue volume >16.3 mm^3 (OR, 4.42), all $P < 0.001$, and high-risk plaque features ≥2 (OR, 2.70, $P = 0.009$) were independent predictors of OCT-derived vulnerable plaques. The average time for automatic CCTA plaque quantification was 1.8 min per patient.

Conclusion The novel AI-powered method facilitated fully automatic plaque quantification and correlated well with co-registered OCT.

* Corresponding author. Tel: +86 21 62932631, Fax: +86 021 62932631, Email: sxtu@sjtu.edu.cn; Tel: +86 21 62932156, Fax: +86 21 62932156, Email: chumiao@sjtu.edu.cn
†These authors contributed equally to the article.

Graphical abstract

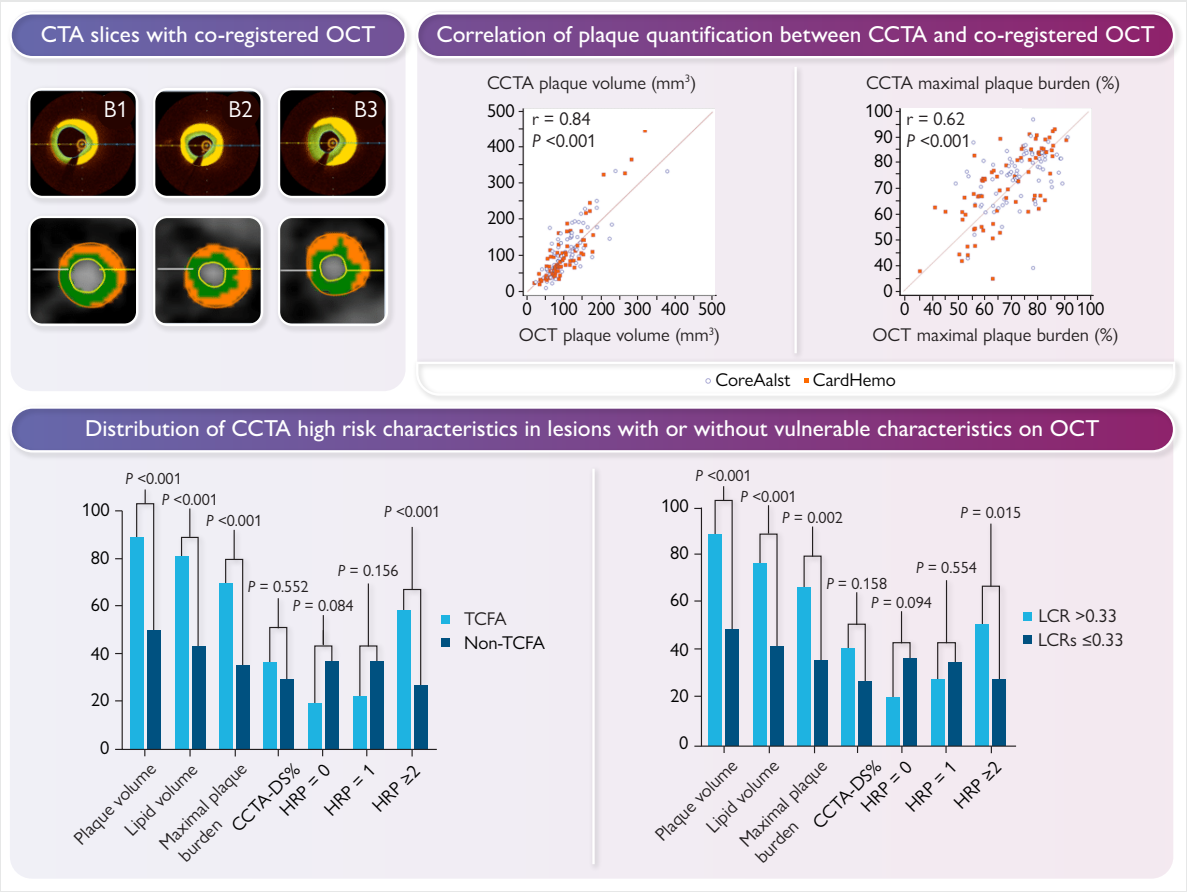

Keywords Coronary computed tomography angiography • Optical coherence tomography • Plaque characterization • Artificial intelligence • Automatic co-registration • Plaque vulnerability

Introduction

Coronary computed tomography angiography (CCTA) is a non-invasive imaging tool enabling direct visualization of coronary stenosis and shows high sensitivity in detecting coronary artery disease.[1] In addition, CCTA also permits the quantification of total plaque volume and the detection of plaque subtypes including calcified, non-calcified, and low attenuation plaque,[2,3] providing incremental prognostic value beyond luminal stenosis.[4,5] However, accurate plaque quantification and characterization from CCTA remains challenging due to the relatively modest Hounsfield unit (HU) difference between noncalcified plaque composition and perivascular adipose tissue[6] and variable plaque attenuation dependent on transluminal attenuation.[7] More importantly, manual delineation or modification is frequently required in conventional visual or semi-automatic CCTA plaque quantification, making the analysis process time-consuming, expertise-dependent, and often poorly reproducible.

The application of artificial intelligence (AI) has largely facilitated lumen and plaque quantification on CCTA with higher accuracy and efficiency when compared with expert readers or intravascular ultrasound (IVUS).[8–12] However, current AI-assisted plaque quantification have certain limitations as requiring predefined coronary artery centerline[8] or focusing simply on segment-level classification,[10] and individual components classification of noncalcified plaque remained challenging.[9,12] As such, we proposed a fully automatic, end-to-end plaque quantification and characterization method with AI-powered lumen and vessel segmentation followed by adaptive HU thresholds for detailed classification of different plaque compositions on CCTA. The aim of this study was to evaluate the performance of the proposed method for CCTA image interpretation with intravascular optical coherence tomography (OCT), a high-resolution, catheter-based imaging modality capable of investigating detailed coronary plaque characterization,[13,14] as the reference standard. In order to have precise comparison between CCTA and OCT, a dedicated algorithm was applied for automatic co-registration between CCTA and OCT, with the link of coronary angiography.

Methods

Study population

This was a retrospective study including patients who had undergone CCTA and coronary catheterization with invasive coronary

angiography (ICA) and OCT imaging prior to any intervention between February 2019 and September 2023. Major inclusion criteria were (i) CCTA, ICA, and OCT images acquired within 6 months; (ii) having ≥1 lesion with at least 30% diameter stenosis by visual estimation in a major epicardial coronary artery on CCTA; and (iii) nitroglycerine administrated prior to CCTA and ICA image acquisitions. All imaging data fulfilling the inclusion criteria at two core labs (CardHemo, Med-X Research Institute, Shanghai Jiao Tong University, Shanghai, China; CoreAalst BV, OLV Clinic, Aalst, Belgium) were screened. The institutional review boards or ethics committees of the hospitals which provided the datasets to the two core labs approved the *post hoc* analysis of these data and all patients provided written informed consent. All imaging data were fully anonymized before being transferred to be analysed at the CardHemo core lab (Med-X Research Institute, Shanghai Jiao Tong University, Shanghai, China).

Patients were excluded from the core lab analysis if they had (i) poor CCTA image quality including image noise and motion artefacts; (ii) insufficient CCTA image spatial resolution; or (iii) poor OCT image quality including insufficient vessel visibility and artefacts.

Image acquisition

Five different CT scanners were used to acquire CCTA images: a 256-rows CT scanner (Revolution CT, GE Healthcare, Fairfield, USA), a dual-source CT scanner (Somatom Force, Siemens, Forchheim, Germany), a dual-source CT scanner (Somatom Definition Flash, Siemens, Forchheim, Germany), a 256-rows CT scanner (iCT 256, Philips Healthcare, Amsterdam, The Netherlands), and a 320-rows CT scanner (Acquisition One, Toshiba, Otawara, Japan). The acquisition was performed following the routine clinical practice and the quality standard set by the Society of Cardiovascular Computed Tomography, with the recommendation of routine sublingual nitrates and oral or intravenous β-blocker when appropriate for targeting a heart rate of ≤60 bpm.[15] ICA was performed by a monoplane or biplane X-ray system. Angiographic images were acquired at 15 frames/s following standard procedures. OCT pullbacks were acquired by the OPTIS® system (Abbott Vascular, Santa Clara, USA). The fibre probe was pulled back within the stationary imaging sheath. Cross-sectional images were generated at a rotational speed of 100 or 180 frames/second. The pull back length was 54 or 75 mm and the frame pitch was 100 or 200 μm. All images were digitally recorded and stored in DICOM format.

CCTA image analysis

CCTA images were analysed using an in-house developed prototype software (INVESSEL, CIIIC lab, Shanghai Jiao Tong University). The fully automatic assessment of coronary lumen and plaque for total plaque quantification, and pixel-wise classification of plaque compositions on CCTA was performed in a coarse-to-fine scheme using a multi-task 3D U-Net, a fully convolutional regression network, and adaptive HU thresholds method (*Figure 1*), detailed analysis pipeline and adaptive threshold methodology were described in the Supplementary Appendices. The developed lumen and vessel wall segmentation method has been integrated in the commercial software (CtaPlus, Pulse Medical, Shanghai, China) for computation of CT-μFR.[16] In addition, qualitative high-risk plaque (HRP) features including positive remodelling, low-attenuation plaque, spotty calcification, and the napkin-ring sign were identified at the core lab by two certified analysts.[17] A plaque with at least 2 HRP features were identified as HRP. More details regarding CCTA image analysis, high risk plaque definition and plaque quantification metrics are included in the Supplementary Appendices.

OCT image analysis

OCT analysis was performed by an independent analyst not involved in CCTA analysis, using a dedicated and validated AI-powered software (OctPlus, version V2, Pulse Medical, Shanghai, China), as described previously.[13,18,19] Lumen contours and internal elastic lamina delineation and plaque characterization were automatically performed using an AI model. The AI model has been validated with good accuracy for plaque characterization and quantification of plaque burden by incorporating the information from adjacent OCT cross-sections and the prior knowledge of the shape of internal elastic lamina.[13,20] The plaque was characterized as lipidic, fibrous or calcified composition on each cross-section of OCT pullback (*Figure 1*). The region without optical signal behind the guidewire was not assigned to any specific plaque composition, however, it was included in the calculation of plaque volume which was defined by the volume of all the tissues between the lumen and internal elastic lamina. Thin-cap fibroatheroma (TCFA) was defined as maximal lipid angle >90° and fibrous cap thickness ≤65 μm.[21] Beside TCFA, plaque vulnerability on OCT is also assessed by lipid-to-cap ratio (LCR), which was found as a strong predictor of non-culprit vessel-related major adverse cardiovascular events in ACS patients.[18] LCR was automatically calculated as the ratio of lipid burden to fibrous cap thickness on every cross-section based on plaque characterization (*Figure 2*). Lesion-level LCR was defined as the maximal LCR along the stenotic segment. Of note, LCR was found as a strong predictor of non-culprit vessel-related major adverse cardiovascular events in ACS patients.[18]

Co-registration comparison

Interrogated lesions were automatically co-registered between CCTA and OCT with the link of ICA (*Figure 1*). A validated co-registration algorithm was used to perform automatic co-registration between ICA and OCT based on lumen contour and side branches on both modalities, and provided the position of every OCT cross-section on the angiographic centreline.[22,23] Then, a graph neural network-based vessel matching network, called GVM-Net,[24] was used to automatically co-register coronary artery centrelines between CCTA and ICA, and had been incorporated in the prototype software for CCTA analysis (INVESSEL, CIIIC lab, Shanghai Jiao Tong University). Finally, each OCT cross-section was matched with an arterial centreline point on CCTA. Cross-modality comparison for the quantifications of total plaque and each individual composition was performed on lesion with at least 30% diameter stenosis on CCTA. The definitions of quantitative plaque parameters on CCTA and OCT were described in the Supplementary Appendices. The length-dependent measurements including plaque volume, lumen volume and specific plaque component volume were corrected when the paired lesion differed in length.

Statistical analysis

Data were analysed on a per-lesion basis. Continuous variables are presented as mean ± standard deviation if normally distributed or otherwise as median (interquartile range) and categorical variables are presented as frequency and percentage. Comparisons between CCTA and OCT measurements were performed using paired Student's t test. The correlation and agreement of quantification results between the two modalities were determined by Pearson's correlation coefficient and Bland–Altman plot, respectively. The diagnostic performance of the CCTA-derived parameters for identifying vulnerable plaque was assessed by receiver operating characteristic analysis and the optimal cutoffs were determined by maximizing Youden index. Qualitative and binary quantitative plaque parameters from CCTA were correlated to vulnerable plaque characteristics on OCT using generalized estimation equations with a logit link function. One-way analysis of variance was done to investigate the variability of the scanner type in CCTA-derived plaque volume. Cohen's kappa coefficient was used to assess inter-observer variability in qualitative high-risk plaque features measurements.

All statistical analyses were performed using MedCalc Statistical Software (version 14.12.0, SPSS Inc, Chicago, IL, USA) and SPSS (version 27, IBM Corp., Armonk, NY, USA). A two-sided *P* value of <0.05 was considered to be statistically significant.

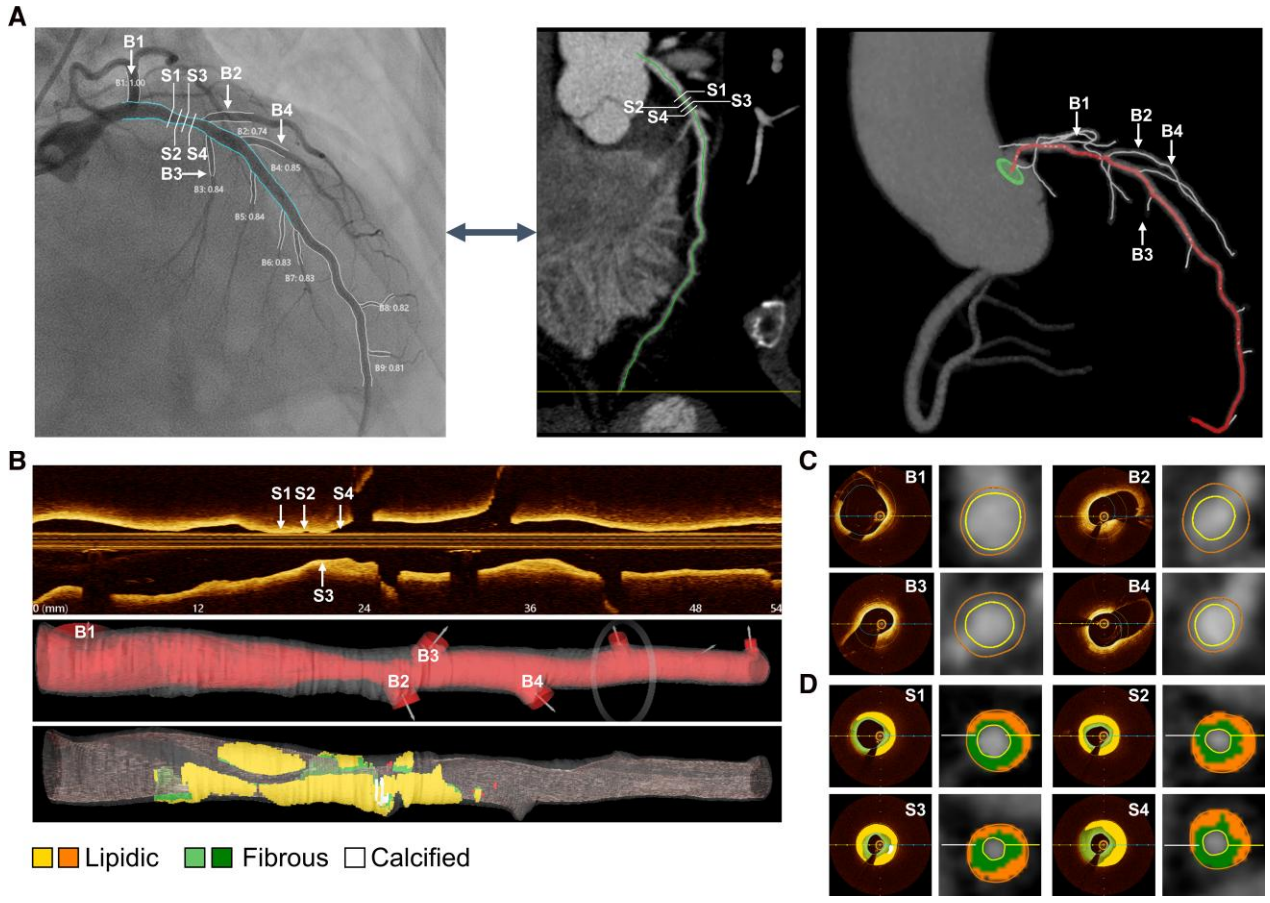

Figure 1 A representative case illustrating co-registration between CCTA and OCT with the link of ICA and plaque identification on OCT and CCTA. (*A*) ICA, curved planar reformation and maximum projection view of CCTA show a moderate stenosis in the LAD of a 63-years-old male patient with unstable angina. Co-registration of centrelines derived from ICA and CCTA was performed to enable point-to-point matching. (*B*) Corresponding longitudinal view, 3D reconstruction with lumen contours and internal elastic lamina delineation and 3D reconstruction with colour-coded plaque from the OCT pullback provide a visual representation of the stenosis and plaque information. (*C*) Cross-sections of corresponding branches on OCT and CCTA; (*D*) Plaque characterization on cross-sections of OCT and CCTA within the lesion at the proximal segment. CCTA, coronary computed tomography angiography; ICA, invasive coronary angiography; LAD, left anterior descending artery; OCT, optical coherence tomography; 3D, 3-dimensional.

Results

Patient population and lesion characteristics

A total of 95 patients were screened. Fully automatic CCTA analysis and co-registration with OCT were successfully performed in 153 coronary lesions from 91 patients (*Figure 3*). Baseline demographic and lesion characteristics are summarized in *Table 1*. The mean age of the patients was 63.6 ± 9.4 years, 70 (76.9%) were male, 25 (27.5%) were with silent ischaemia, 48 (52.7%) were with stable angina and 17 (18.7%) were diagnosed with acute coronary syndrome. Of the 91 patients, 77 (84.6%) underwent CCTA within 3 months, and 48 (52.7%) underwent CCTA within 30 days prior to OCT. Of the 153 target lesions, 108 (70.6%) were located in the left anterior descending, 17 (11.1%) in the left circumflex, and 28 (18.3%) in the right coronary artery. The median lesion length and DS% by quantitative angiography were 15.7 mm (interquartile range, 12.5–20.5 mm) and 40.0% (interquartile range, 30.0–51.0%), respectively. Vulnerable plaque with LCR >0.33 was observed in 39 (25.5%) and TCFA in 36 (23.5%) interrogated lesions.

Comparison of lumen and plaque quantification between CCTA and OCT

CCTA and OCT-derived lumen and plaque characteristics are summarized in *Table 2*. CCTA images were obtained on CT scanners from four different vendors (Toshiba, $n = 18$; Philips, $n = 12$; GE, $n = 15$; and Siemens, $n = 46$). For lumen quantification, the minimal lumen area and lumen volume were smaller by CCTA than by OCT, being 2.5 ± 1.3 mm^2 vs. 2.9 ± 2.0 mm^2 ($P < 0.001$) and 69.4 ± 33.1 mm^3 vs. 97.2 ± 49.0 mm^3 ($P < 0.001$), respectively. There were good correlations for both minimal lumen area ($r = 0.80$, $P < 0.001$) and lumen volume ($r = 0.84$, $P < 0.001$) between the two modalities. Plaque quantification demonstrated similar plaque volume between the two modalities (110.6 ± 72.9 mm^3 vs. 105.3 ± 54.6 mm^3, $P = 0.100$) (*Figure 4*).

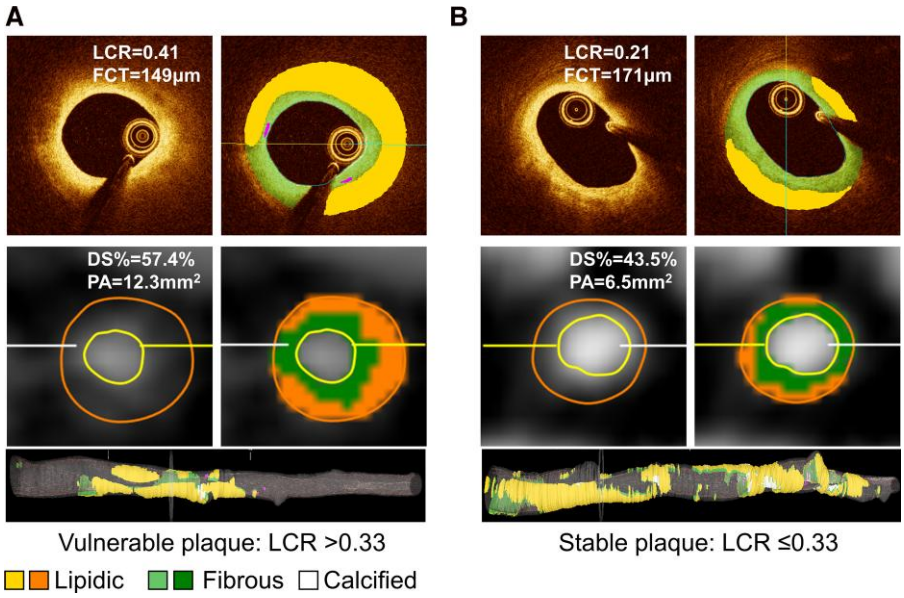

Figure 2 Representative examples of morphological assessment of vulnerable and stable plaque. (*A*) The OCT cross-section imaged from a 63-year-old male patient with unstable angina shows a vulnerable plaque with LCR >0.33 and the corresponding CCTA cross-section reveals a large plaque area and lipidic plaque area. (*B*) The OCT cross-section imaged from an 83-year-old female patient with stable angina shows a stable plaque with LCR <0.33 and the corresponding CCTA cross-section shows a small lipidic plaque area. The overall plaque distribution is presented by the 3D reconstruction of OCT with colour-coded plaque. DS%, percent diameter stenosis; FCT, fibrous cap thickness; LCR, lipid-to-cap ratio; PA, plaque area. Other abbreviations as in *Figure 1*.

Maximal plaque burden was slightly overestimated by CCTA compared with OCT with a mean difference of 1.9% (P = 0.028). Good correlation for plaque volume (r = 0.84) and moderate correlation for maximal plaque burden (r = 0.62) were observed between CCTA and OCT (all P values <0.001). One-way analysis of variance showed no significant difference across CT scanners in evaluating plaque volume compared with OCT (P = 0.102).

Comparison of plaque characterization between CCTA and OCT

AI-powered CCTA analysis showed good agreement of lipidic tissue volume quantification with OCT (24.8 ± 26.8 mm^3 vs. 26.6 ± 22.3 mm^3, P = 0.257) (*Table 2*, *Figure 5*). By contrast, CCTA reported larger volume in both fibrous (70.6 ± 37.7 mm^3 vs. 56.1 ± 26.6 mm^3, P < 0.001) and calcified tissue (15.3 ± 25.5 mm^3 vs. 6.3 ± 9.1 mm^3, P < 0.001). Pearson's correlation analysis demonstrated moderate to good correlation of CCTA with OCT for fibrous (r = 0.65), lipidic (r = 0.70), and calcified (r = 0.83) tissue volume (all P values <0.001).

Subgroup analysis of patients with image acquisition interval within 30 days

Seventy-five (49.0%) lesions from 48 patients underwent CCTA prior to OCT within 30 days. The correlation and agreement between CCTA and OCT-derived lumen and plaque quantification metrics were similar in the group within 30 days and total group, with no significant differences (see Supplementary material online, *Tables S1* and *S2*).

Associations of CCTA-derived parameters with plaque vulnerability on OCT

With receiver operating characteristic analysis, plaque quantification parameters, including plaque volume, lipidic tissue volume, and maximal plaque burden, but not DS%, were found to be predictive of vulnerable plaques with either LCR >0.33 or the presence of TCFA (all P values <0.001; Supplementary material online, *Figure S1*). The sensitivity and specificity of plaque volume for identifying LCR >0.33 was 89.7% (35/39) and 51.8% (59/114), respectively, with an area under the curve of 0.73 (95% CI: 0.65, 0.79; Supplementary material online, *Table S3*). Plaque volume >82.5 mm^3 (odds ratio [OR], 9.39; 95% CI: 3.13, 28,14; P < 0.001), maximal plaque burden >76.4% (OR, 3.70; 95% CI: 1.72, 7.98; P < 0.001), and lipidic tissue volume >16.3 mm^3 (OR, 4.42; 95% CI: 1.92, 10.16; P < 0.001) were all significantly associated with LCR >0.33 (*Table 3*). Significant associations with LCR >0.33 were also found for qualitative HRP features (P < 0.05), excepted for spotty calcification. The presence of CCTA-derived HRP (≥2 features) was observed in 52 (34.0%) lesions and was associated with a 2.7-fold risk of LCR >0.33 (P = 0.009). Similar associations were found for these CCTA metrics with TCFA on OCT. Distributions of quantitative and qualitative CCTA characteristics between lesions with and without OCT-identified vulnerable plaques are illustrated in *Graphical Abstract*.

Interobserver variability of qualitative CCTA high risk plaque features

Repeated CCTA-derived HRP features analysis was performed on all lesions. The interobserver kappa coefficient were 0.80

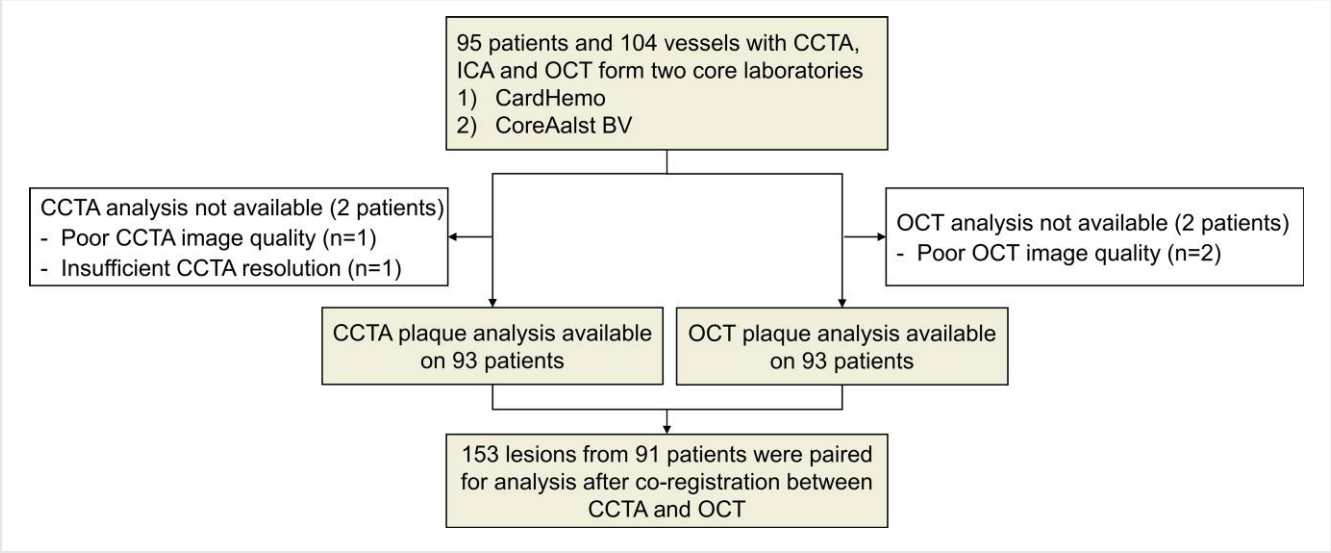

Figure 3 Study flowchart. CCTA, coronary computed tomography angiography; ICA, invasive coronary angiography; OCT, optical coherence tomography.

for positive remodelling, 0.82 for low-attenuation plaque, 0.84 for spotty calcification, 0.74 for napkin-ring sign, and 0.79 for CCTA-derived HRP (≥2 features), respectively.

CCTA analysis duration

The average time for automated CCTA analysis, including image import, lumen and vessel segmentation, plaque quantification, and three-dimensional reconstruction was 1.8 ± 0.4 min per patient on a computer equipped with an Intel Core i7-11700K processor, 32GB random access memory and a NVIDIA RTX A4000 graphics card.

Discussion

To our best knowledge, this is the first study reporting the performance of an end-to-end automated CCTA plaque analysis with comparison to OCT, enhancing by co-registration software for accurate lesion matching between CCTA and OCT. The main findings of this study are as follows: (i) Fully automatic plaque characterization of CCTA and co-registration with ICA and OCT is feasible; (ii) Automatic CCTA-derived plaque volume showed good correlation and agreement with OCT; (iii) For specific plaque composition, there was moderate-to-good correlation between CCTA and OCT for lipidic tissue volume, while fibrous and calcified tissue volume were overestimated by CCTA; (iv) CCTA-derived plaque volume appeared superior to other quantitative parameters and HRP for the prediction of vulnerable plaques on OCT; and (v) the analysis time required for the AI-assisted fully automatic plaque characterization on CCTA images was less than 2 min on an off-the-shelf computer.

During the past decade, AI has been increasingly applied to assist medical image analysis, including CCTA, by improving efficiency and accuracy.[25] For plaque analysis, AI was mostly used for lumen and wall segmentation, rarely for plaque composition classification due to difficulty of precise pixel-level plaque composition labelling. A recent deep-learning model trained by Lin *et al.*[8] showed high feasibility in automatic plaque quantification from CCTA through a ConvLSTM-based neural network in a multicentre cohort. However, this method still required predefined centreline and classified plaques into calcified and non-calcified subtype by adaptive HU threshold.[8] Furthermore, manual registration was needed for cross-modality comparison in this study, which might result in inaccurate alignment between CCTA and the reference standard. Ramasamy *et al.*[9] generated plaque composition label by projecting matched near-infrared spectroscopy IVUS onto CCTA slices for training AI model. However, the correlation of plaque volume was fair (intra-class correlation coefficient = 0.52, $P < 0.001$). Accordingly, adaptive HU threshold would still be a preferable choice for plaque composition classification, and current study extended it for further distinguishing non-calcified plaque into lipidic and fibrous compositions. Of note, our novel AI-enabled method allows automatic plaque quantification and more detailed characterization of different plaque compositions without any additional manual interference. The AI models were developed using a dataset from our core laboratory (CardHemo, Shanghai Jiao Tong University), entirely independent from the current study population. This separation is crucial for avoiding data leakage and overfitting risk. Meanwhile, the performance of the AI models for lumen and vessel wall segmentation was externally validated for CT-μFR computation in the CAREER study.[26] Fully-automated CT-μFR analysis based on the above AI models maintained high diagnostic accuracy (83.0%) in comparison with semi-automatic analysis with manual correction (89.6%), indicating robust external performance and low overfitting risk. Following AI-enabled automatic processing of plaque characterization on OCT[13] and co-registration between CCTA and OCT with the link of ICA,[23] our proposed method demonstrated good agreement with the reference standard regarding both plaque quantification and characterization. The fully automatic process further reduced the associated time consumption (1.8 min vs. 3.8 min).[8] These features support large scale analysis for future clinical investigations of CCTA images.

CCTA-based plaque quantification

Multiple imaging modalities have been used for atherosclerosis plaque assessment.[27] Specifically, IVUS is widely used as a

Table 1 Baseline patient and lesion characteristics

Baseline characteristics	
All patients (n = 91)	
Male	70 (76.9)
Age (yr)	63.6 ± 9.4
Body mass index (kg/m^2)	25.2 (23.5, 28.1)
Diabetes mellitus	28 (30.8)
Hypertension	57 (62.6)
Hyperlipidaemia	68 (74.7)
Current smoker	26 (28.6)
Previous PCI	9 (9.9)
Clinical presentation	
Silent ischaemia	25 (27.5)
Stable angina	48 (52.7)
Unstable angina	16 (17.6)
Non-ST-elevation myocardial infarction	1 (1.1)
Others	1 (1.1)
All lesions (n = 153)	
Target lesion location	
Left anterior descending artery	108 (70.6)
Diagonal artery	1 (0.7)
Left circumflex artery	17 (11.1)
Right coronary artery	28 (18.3)
Quantitative coronary angiography	
Minimal lumen diameter (mm)	1.7 (1.5, 2.2)
DS% (%)	40.0 (30.0, 51.0)
Lesion length (mm)	15.7 (12.5, 20.5)
OCT measurement	
LCR	0.21 (0.12, 0.35)
LCR > 0.33	39 (25.5)
TCFA	36 (23.5)
CCTA measurement	
Calcified lesion	107 (69.9)
Presence of HRP features	
0	50 (32.7)
1	51 (33.3)
≥2	52 (34.0)

Data are presented as mean ± standard deviation, median [interquartile range], or n (%).
CCTA, coronary computed tomography angiography; DS%, percent diameter stenosis; LCR, lipid-to-cap ratio; OCT, optical coherence tomography; PCI, percutaneous coronary intervention; TCFA, thin-cap fibroatheroma

Table 2 Comparison of lumen and plaque quantifications between CCTA and OCT on lesion level

	OCT	CCTA	*P* value
Lumen quantification			
Minimal lumen area (mm^2)	2.9 ± 2.0	2.5 ± 1.3	<0.001
Lumen volume (mm^3)	97.2 ± 49.0	69.4 ± 33.1	<0.001
Plaque quantification			
Plaque volume (mm^3)	105.3 ± 54.6	110.6 ± 72.9	0.100
Maximal plaque burden (%)	71.0 ± 11.5	72.9 ± 12.7	0.028
Specific plaque composition			
Fibrous tissue volume (mm^3)	56.1 ± 26.6	70.6 ± 37.7	<0.001
Lipidic tissue volume (mm^3)	26.6 ± 22.3	24.8 ± 26.8	0.257
Calcified tissue volume (mm^3)	6.3 ± 9.1	15.3 ± 25.5	<0.001

Data are presented as mean ± standard deviation.
Abbreviations as in *Table 1*.

reference standard in CCTA plaque studies due to its superior penetration depth. However, IVUS has notable limitations in calcified plaque assessment, where calcium shadowing restricts visualization of plaque borders and surrounding tissue structures. OCT offers complementary strengths, including high spatial resolution and excellent visualization of luminal plaque morphology without interference from calcification. However, OCT's limited penetration leads to challenges in far-field plaque boundaries, especially for large plaque volume or heavy lipid content. To address OCT's penetration limitations, we employed a validated algorithm designed to extrapolate invisible portions of the IEL by integrating information from adjacent image frames and applying prior knowledge of vessel geometry.[13] The model's validity has been established through external validation against expert consensus, cross-validation with IVUS, and validation against histology.[13,20]

Plaque quantification represents a basic aspect of CCTA imaging analysis and shows a good correlation with IVUS especially when an AI-powered semi-automatic or automatic method is applied.[8,9,28] Specifically, total and non-calcified plaque volume have been recognized as independent predictors of subsequent acute coronary events,[4,8] which are even more pronounced than stenotic severity and qualitative HRP features.[4] Similarly, our findings of a good correlation with OCT and the strongest association with vulnerable plaques for CCTA-derived plaque volume were consistent with previous observations.[4,8]

In the comparative analysis of volumetric data, a systematic discrepancy was observed between OCT and CCTA lumen volumes, which is attributable to inherent modality-specific characteristics. CCTA may underestimate the lumen due to blooming and partial-volume effects, whereas OCT may overestimate dimensions due to non-coaxial catheter alignment, which produces oblique imaging rather than true short-axis cross-sections. Despite this, the key parameter for clinical decision-making of MLA demonstrated a strong correlation (r = 0.80) between the two modalities. Furthermore, the oblique OCT cross-section affect the lumen and vessel volume simultaneously, therefore the total plaque volumes of OCT remain numerically similar to that of CCTA. Finally, it should be noted that the summation of individual OCT tissue components is smaller than the total plaque volume because guidewire shadow precludes tissue classification in that specific sector.

CCTA-based characterization of specific plaque compositions

Aside from the estimation of total plaque volume, coronary plaques can be further classified as calcified, non-calcified, or low-attenuation subtype according to the predefined HU thresholds on CCTA.[17] However, further characterization of individual plaque compositions of non-calcified plaque from CCTA can be challenging mainly because of the limited spatial resolution of conventional CT scanners. In addition, partial volume effect

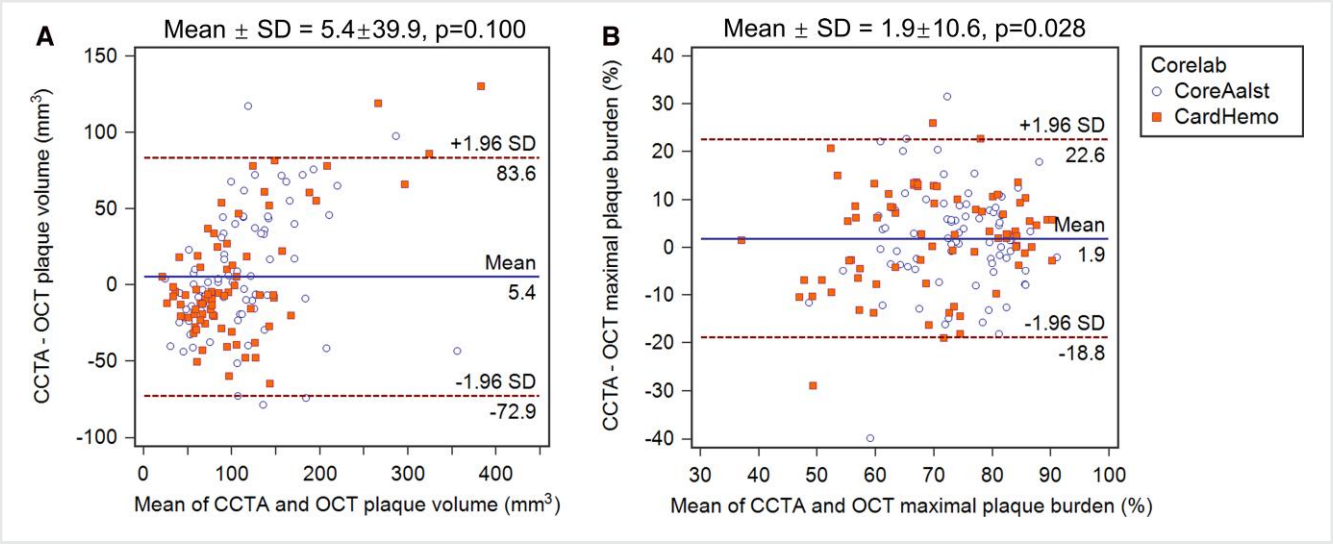

Figure 4 Lesion-level agreement of plaque quantification. For total plaque quantification, CCTA showed good agreement with OCT for plaque volume (*A*), and moderate agreement for maximal plaque burden (*B*). Abbreviations as in *Figure 1*.

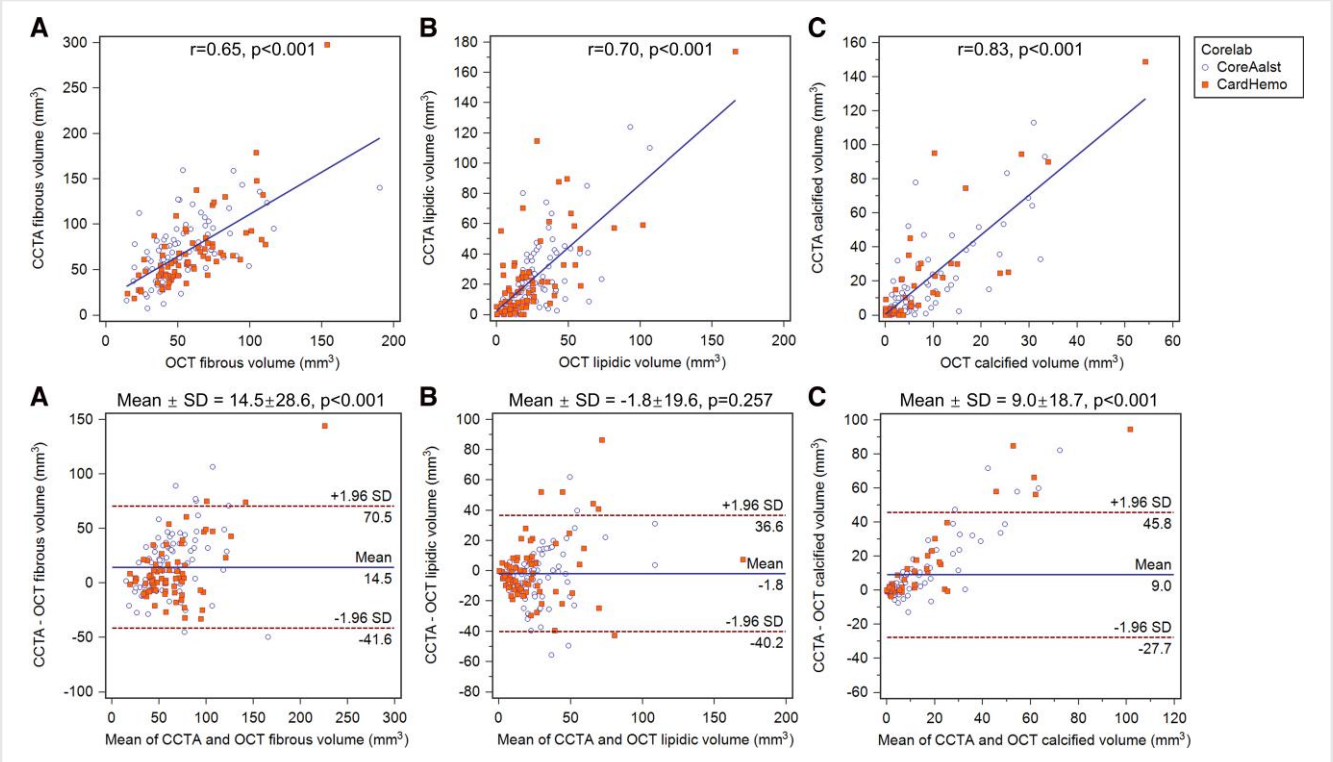

Figure 5 Lesion-level correlation and agreement of specific plaque compositions quantification. As to the characterization of different plaque compositions, moderate correlation and agreement was observed for fibrous (*A*), and moderate correlation and good agreement was observed for lipidic volume (*B*), and good correlation and moderate agreement for calcified volume (*C*) between CCTA and OCT. Abbreviations as in *Figure 1*.

caused by calcified plaque and variable HU thresholds due to intracoronary contrast attenuation may also lead to frequent misclassification of different plaque compositions.[27,29] In this study, an AI-enabled method with adaptive HU thresholds was applied for automatic and detailed plaque characterization by further differentiating lipidic tissue from non-calcified plaque. Although there was an overall acceptable correlation and agreement with OCT, the performance of plaque characterization on

Table 3 Associations of CCTA-derived parameters with vulnerable plaque characteristics on OCT

	Crude OR (95% CI)	*P* value	Adjusted OR (95% CI)	*P* value
TCFA				
DS% >50.0%	1.17 (0.45, 3.04)	0.746	1.17 (0.46, 3.02)	0.744
Plaque volume >82.5 mm^3	8.14 (2.71, 24.47)	<0.001	8.14 (2.69, 24.61)	<0.001
Maximal plaque burden >76.4%	4.21 (1.89, 9.42)	<0.001	4.21 (1.82, 9.74)	<0.001
Lipidic tissue volume >16.3 mm^3	5.55 (2.25, 13.70)	<0.001	5.55 (2.02, 15.27)	<0.001
Qualitative HRP features				
Positive remodelling	4.02 (1.74, 9.30)	0.001	4.02 (1.70, 9.49)	0.002
Low-attenuation plaque	2.60 (1.16, 5.85)	0.021	2.60 (1.11, 6.09)	0.028
Napkin-ring sign	4.54 (1.60, 12.87)	0.004	4.54 (1.49, 13.86)	0.008
Spotty calcification	1.67 (0.77, 3.62)	0.191	1.67 (0.82, 3.42)	0.159
HRP features ≥2	3.88 (1.78, 8.47)	<0.001	3.88 (1.77, 8.52)	<0.001
LCR >0.33				
DS% >50.0%	1.60 (0.65, 3.93)	0.306	1.60 (0.66, 3.88)	0.299
Plaque volume >82.5 mm^3	9.39 (3.13, 28.14)	<0.001	9.39 (3.21, 27.48)	<0.001
Maximal plaque burden >76.4%	3.70 (1.72, 7.98)	<0.001	3.70 (1.64, 8.36)	0.002
Lipidic tissue volume >16.3 mm^3	4.42 (1.92, 10.16)	<0.001	4.42 (1.89, 10.38)	<0.001
Qualitative HRP features				
Positive remodelling	3.38 (1.53, 7.44)	0.003	3.38 (1.57, 7.28)	0.002
Low-attenuation plaque	2.61 (1.18, 5.79)	0.018	2.61 (1.19, 5.76)	0.017
Napkin-ring sign	3.01 (1.07, 8.46)	0.037	3.01 (1.00, 9.04)	0.050
Spotty calcification	1.21 (0.57, 2.61)	0.620	1.21 (0.59, 2.48)	0.596
HRP features ≥2	2.70 (1.28, 5.71)	0.009	2.70 (1.22, 6.00)	0.014

Optimal cutoffs were determined by ROC analysis and maximal Youden index.
CI, confidence interval; OR, odds ratio; other abbreviations as in *Table 1*.

CCTA varied substantially among major plaque compositions, with minor bias observed for lipidic while significant overestimation for both fibrous and calcified tissue volume. This might be explained by calcium blooming and the inclusion of media into the estimation of total and fibrous tissue volume on CCTA. Meanwhile, the area blocked by the guidewire artefact on OCT had been waived for plaque characterization, which might also partially account for the overestimation of plaque compositions by CCTA when using OCT as the gold standard. Notwithstanding these systemic biases, comparable performance of our method for lipidic quantification to OCT should have prognostic implications since lipidic plaque is more clinically relevant as compared with fibrous or calcified plaque.

Potential clinical applications of automated CCTA plaque analysis

With use of the novel AI-powered method, CCTA-derived plaque quantification and characterization parameters, especially plaque volume ($r = 0.84$), correlated well with OCT (all $P < 0.001$). The strongest predictor of OCT-derived vulnerable plaques was found for CCTA-derived plaque volume >82.5 mm^3 (odds ratio, 9.39; $P < 0.001$), potentially due to its higher correlation with OCT compared with specific plaque types. In contrast, spotty calcification is the weakest predictor of OCT-identified TCFA. This AI-powered method enabled fully automatic and fast plaque quantification and characterization from CCTA with a mean analysis time of 1.8 min per patient and could support the utility of plaque analysis in patients underwent CCTA. To be noted, the patient population in the present study presented more severe coronary artery disease than cohorts typically enrolled in diagnostic CCTA registries. This is because all included patients were referred to the catheterization laboratory for clinically indicated invasive coronary angiography and was subsequently followed by OCT examination. The demonstrated performance of the proposed algorithm on these advanced, complex lesions supports its potential for clinical generalizability to the less severe lesions typically encountered in routine diagnostic CCTA practice.

Limitations

The current study has several limitations. First, this is a post-hoc analysis with a relatively small sample size. Further prospective studies are warranted to assess the performance of this novel AI method for CCTA interpretation. Second, although the AI-powered method for fully automatic CCTA analysis showed significant correlations for plaque volume and composition quantification compared with OCT, the overall accuracy for plaque composition classification was modest. This might be due to the intrinsic differences between CCTA and OCT imaging as well as the shadow caused by guidewire artefact on OCT. Inherent mismatch of image slice between CCTA and OCT would be introduced by different inter-slice distance of OCT (typically 0.2 mm) and CCTA (typically 0.6 mm). Besides, the matched slice of CCTA and OCT would share different imaging plane due to the misalignment of OCT catheter orientation and CCTA vessel centreline orientation. This would affect the

slice-by-slice comparison including maximal plaque burden. The study observed a higher proportion of lipidic plaque, potentially due to imperfect segmentation of the outer vessel wall, where the blurry boundary with epicardial fat may lead to overestimation of lipidic plaque volume on CCTA. Additionally, CCTA images were acquired from different CT scanners following heterogeneous protocols. Further investigations are needed to validate the efficacy of this method in CCTA images acquired following a standardized protocol. Fourth, vessels with stent implantation were excluded from model training. The performance of this method in stented vessels remains largely unknown. Fifth, unlike plaque quantification, HRP features were manually or semi-automatically qualified in our study. Automatic assessment of these qualitative high-risk features will be warranted and integrated into the dedicated software. Finally, the optimal cutoffs determined by the Youden Index were not validated in an independent holdout test set. Therefore, larger, independent validation is needed before clinical application.

Conclusions

The novel AI-powered method enabled rapid and fully automatic end-to-end plaque quantification and characterization with moderate-to-good accuracy compared with co-registered OCT. Plaque volume assessed by this approach showed the potential to predict OCT-derived vulnerable plaques.

Lead author biography

Guanyu Li is a PhD student under supervision of Prof. Shengxian Tu, in the Biomedical Instrument Institute, School of Biomedical Engineering, Shanghai Jiao Tong University, Shanghai, China. His research focuses on developing CCTA-based evaluation methods for cardiovascular diseases, including CT-μFR and atherosclerotic plaque quantification.

Supplementary material

Supplementary material is available at *European Heart Journal – Digital Health*.

Acknowledgements

The authors would like to thank the CoreAalst BV for providing data.

Author contributions

Guanyu Li (BSc (Investigation [equal]; Methodology [equal]; Writing—original draft [lead])), Wei Yu (PhD (Investigation [equal]; Methodology [equal]; Software [equal])), Zhiqing Wang (MD PhD (Formal analysis [equal]; Validation [equal])), Yankai Chen (BSc (Methodology [equal]; Software [equal])), Miao Chu (PhD (Funding acquisition [equal]; Supervision [equal]; Writing—original draft [equal]; Writing—review & editing [lead])), Zehang Li (PhD (Methodology [supporting]; Software [supporting]; Validation [equal])), Chunming Li (BSc (Methodology [supporting]; Software [supporting]; Validation [equal])), Xiaoling Wang (MSc (Validation [equal])), Yuanming Yan (MD (Methodology [supporting]; Validation [supporting])), Yukun Luo (MD (Investigation [supporting]; Validation [supporting])), Wei Cai (MD (Data curation [supporting]; Validation [supporting])), Giovanni Luigi De Maria (PhD (Conceptualization [supporting]; Supervision [supporting])), Charalambos Antoniades (MD PhD (Conceptualization [supporting]; Supervision [supporting])), Adrian Banning (MD PhD (Conceptualization [supporting]; Supervision [supporting])), Lianglong Chen (MD PhD (Conceptualization [supporting]; Data curation [supporting]; Supervision [supporting])), and Shengxian Tu (PhD (Conceptualization [lead]; Funding acquisition [lead]; Project administration [lead]; Supervision [lead]; Writing—original draft [equal]; Writing—review & editing [lead]))

Funding

This work is supported by the National Key Research and Development Program of China (2023YFC2506503) and by the National Natural Science Foundation of China (82020108015 and 82302285).

Conflict of interest: S.T. is the cofounder of, has received research grants from, and been a consultant for Pulse Medical. C.A. is the immediate past Chair of the British Atherosclerosis Society, and he is Founder, shareholder and director of Caristo Diagnostics, a University of Oxford Spinout company. C.A. declares honoraria from Amarin, Silence Therapeutics, Abcentra, Amgen and Caristo Diagnostics. All other authors have reported that they have no relationships relevant to the contents of this paper to disclose.

Data availability

Data generated or analysed during the study are available from the corresponding author by reasonable request.

References

1. Vanhoenacker PK, Heijenbrok-Kal MH, Van Heste R, Decramer I, Van Hoe LR, Wijns W, *et al.* Diagnostic performance of multidetector CT angiography for assessment of coronary artery disease: meta-analysis. *Radiology* 2007;**244**:419–428.
2. Boogers MJ, Broersen A, van Velzen JE, de Graaf FR, El-Naggar HM, Kitslaar PH, *et al.* Automated quantification of coronary plaque with computed tomography: comparison with intravascular ultrasound using a dedicated registration algorithm for fusion-based quantification. *Eur Heart J* 2012;**33**:1007–1016.
3. van Rosendael AR, Maliakal G, Kolli KK, Beecy A, Al'Aref SJ, Dwivedi A, *et al.* Maximization of the usage of coronary CTA derived plaque information using a machine learning based algorithm to improve risk stratification; insights from the CONFIRM registry. *J Cardiovasc Comput Tomogr* 2018;**12**:204–209.
4. Andreini D, Magnoni M, Conte E, Masson S, Mushtaq S, Berti S, *et al.* Coronary plaque features on CTA can identify patients at increased risk of cardiovascular events. *JACC Cardiovasc Imaging* 2020;**13**:1704–1717.
5. Williams MC, Kwiecinski J, Doris M, McElhinney P, D'Souza MS, Cadet S, *et al.* Low-attenuation noncalcified plaque on coronary computed tomography angiography predicts myocardial infarction: results from the multicenter SCOT-HEART trial (Scottish Computed Tomography of the HEART). *Circulation* 2020;**141**:1452–1462.
6. de Knegt MC, Haugen M, Jensen AK, Linde JJ, Kuhl JT, Hove JD, *et al.* Coronary plaque composition assessed by cardiac computed tomography using adaptive Hounsfield unit thresholds. *Clin Imaging* 2019;**57**:7–14.
7. Bae KT. Intravenous contrast medium administration and scan timing at CT: considerations and approaches. *Radiology* 2010;**256**:32–61.
8. Lin A, Manral N, McElhinney P, Killekar A, Matsumoto H, Kwiecinski J, *et al.* Deep learning-enabled coronary CT angiography for plaque and stenosis quantification and cardiac risk prediction: an international multicentre study. *Lancet Digit Health* 2022;**4**:e256–e265.
9. Ramasamy A, Sokooti H, Zhang X, Tzorovili E, Bajaj R, Kitslaar P, *et al.* Novel near-infrared spectroscopy-intravascular ultrasound-based deep-learning

methodology for accurate coronary computed tomography plaque quantification and characterization. *Eur Heart J Open* 2023;**3**:oead090.
10. Zreik M, van Hamersvelt RW, Wolterink JM, Leiner T, Viergever MA, Isgum I. A recurrent CNN for automatic detection and classification of coronary artery plaque and stenosis in coronary CT angiography. *IEEE Trans Med Imaging* 2019;**38**:1588–1598.
11. Muscogiuri G, Chiesa M, Trotta M, Gatti M, Palmisano V, Dell'Aversana S, *et al.* Performance of a deep learning algorithm for the evaluation of CAD-RADS classification with CCTA. *Atherosclerosis* 2020;**294**:25–32.
12. Lin A, Slomka PJ, Dey D. Artificial intelligence-based evaluation of coronary atherosclerotic plaques. In: De Cecco CN, van Assen M, Leiner T, eds. *Artificial Intelligence in Cardiothoracic Imaging*. Cham: Springer International Publishing; 2022. p259–265.
13. Chu M, Jia H, Gutiérrez-Chico JL, Maehara A, Ali ZA, Zeng X, *et al.* Artificial intelligence and optical coherence tomography for the automatic characterisation of human atherosclerotic plaques. *EuroIntervention* 2021;**17**:41–50.
14. Araki M, Park SJ, Dauerman HL, Uemura S, Kim JS, Di Mario C, *et al.* Optical coherence tomography in coronary atherosclerosis assessment and intervention. *Nat Rev Cardiol* 2022;**19**:684–703.
15. Abbara S, Blanke P, Maroules CD, Cheezum M, Choi AD, Han BK, *et al.* SCCT guidelines for the performance and acquisition of coronary computed tomographic angiography: a report of the society of Cardiovascular Computed Tomography Guidelines Committee: Endorsed by the North American Society for Cardiovascular Imaging (NASCI). *J Cardiovasc Comput Tomogr* 2016;**10**:435–449.
16. Weng T, Ding D, Li G, Guan S, Han W, Gan Q, *et al.* Accuracy of coronary computed tomography angiography-derived quantitative flow ratio for onsite assessment of coronary lesions. *EuroIntervention* 2024;**20**:e1288–e1297.
17. Cury RC, Leipsic J, Abbara S, Achenbach S, Berman D, Bittencourt M, *et al.* CAD-RADS 2.0—2022 coronary artery disease-reporting and data system: an expert consensus document of the Society of Cardiovascular Computed Tomography (SCCT), the American College of Cardiology (ACC), the American College of Radiology (ACR), and the North America Society of Cardiovascular Imaging (NASCI). *JACC Cardiovasc Imaging* 2022;**15**:1974–2001.
18. Hong H, Jia H, Zeng M, Gutierrez-Chico JL, Wang Y, Zeng X, *et al.* Risk stratification in acute coronary syndrome by comprehensive morphofunctional assessment with optical coherence tomography. *JACC Asia* 2022;**2**:460–472.
19. Huang J, Ninomiya K, Tu S, Masuda S, Dijkstra J, Chu M, *et al.* Calcified plaque detected on OCT with deep learning and cross-validated with optical and ultrasound signals: a complementary appraisal and preamble to combined IVUS-OCT catheter. *Front Photon* 2022;**3**:1019552.
20. Huang J, Tu S, Masuda S, Ninomiya K, Dijkstra J, Chu M, *et al.* Plaque burden estimated from optical coherence tomography with deep learning: in vivo validation using co-registered intravascular ultrasound. *Catheter Cardiovasc Interv* 2022;**101**:287–296.
21. Kedhi E, Berta B, Roleder T, Hermanides RS, Fabris E, IJsselmuiden AJJ, *et al.* Thin-cap fibroatheroma predicts clinical events in diabetic patients with normal fractional flow reserve: the COMBINE OCT-FFR trial. *Eur Heart J* 2021;**42**:4671–4679.
22. Ding D, Tu S, Li Y, Li C, Yu W, Liu X, *et al.* Quantitative flow ratio modulated by intracoronary optical coherence tomography for predicting physiological efficacy of percutaneous coronary intervention. *Catheter Cardiovasc Interv* 2023;**102**:36–45.
23. Li C, Qiao Y, Yu W, Li Y, Chen Y, Fan Z, *et al.* AutoFOX: an automated cross-modal 3D fusion framework of coronary X-ray angiography and OCT. *Med Image Anal* 2025;**101**:103432.
24. Chen Y, Li G, Li C, Yu W, Fan Z, Bai J, *et al.* GVM-Net: a GNN-based vessel matching network for 2D/3D non-rigid coronary artery registration. *IEEE Trans Med Imaging* 2025;**44**:2617–2630.
25. Follmer B, Williams MC, Dey D, Arbab-Zadeh A, Maurovich-Horvat P, Volleberg R, *et al.* Roadmap on the use of artificial intelligence for imaging of vulnerable atherosclerotic plaque in coronary arteries. *Nat Rev Cardiol* 2024;**21**:51–64.
26. Li G, Weng T, Sun P, Li Z, Ding D, Guan S, *et al.* Diagnostic performance of fully automatic coronary CT angiography-based quantitative flow ratio. *J Cardiovasc Comput Tomogr* 2025;**19**:40–47.
27. Williams MC, Earls JP, Hecht H. Quantitative assessment of atherosclerotic plaque, recent progress and current limitations. *J Cardiovasc Comput Tomogr* 2022;**16**:124–137.
28. Narula J, Stuckey TD, Nakazawa G, Ahmadi A, Matsumura M, Petersen K, *et al.* Prospective deep learning-based quantitative assessment of coronary plaque by CT angiography compared with intravascular ultrasound. *Eur Heart J Cardiovasc Imaging* 2024;**25**:1287–1295.
29. Cademartiri F, Mollet NR, Runza G, Bruining N, Hamers R, Somers P, *et al.* Influence of intracoronary attenuation on coronary plaque measurements using multislice computed tomography: observations in an ex vivo model of coronary computed tomography angiography. *Eur Radiol* 2005;**15**:1426–1431.